Journal of Electrochemistry

Volume 24
Issue 6 *Special Issue in Honor of Professor Baolian Yi on His 80th Birthday*

2018-12-28

Pd/C Catalysts for CO_2 Electroreduction to CO:Pd Loading Effect

Dun-feng GAO

Cheng-cheng YAN

Guo-xiong WANG
State Key Laboratory of Catalysis, Dalian National Laboratory for Clean Energy, Dalian Institute of Chemical Physics, Chinese Academy of Sciences, Dalian, 116023, China;, wanggx@dicp.ac.cn

Xin-he BAO
State Key Laboratory of Catalysis, Dalian National Laboratory for Clean Energy, Dalian Institute of Chemical Physics, Chinese Academy of Sciences, Dalian, 116023, China;, xhbao@dicp.ac.cn

Recommended Citation

Dun-feng GAO, Cheng-cheng YAN, Guo-xiong WANG, Xin-he BAO. Pd/C Catalysts for CO_2 Electroreduction to CO:Pd Loading Effect[J]. *Journal of Electrochemistry*, 2018 , 24(6): 757-765.
DOI: 10.13208/j.electrochem.180845
Available at: https://jelectrochem.xmu.edu.cn/journal/vol24/iss6/17

DOI: 10.13208/j.electrochem.180845 **Artical ID**:1006-3471(2018)06-0757-09
Cite this: *J. Electrochem.* **2018**, *24*(6): 757-765 **Http**://electrochem.xmu.edu.cn

Pd/C Catalysts for CO_2 Electroreduction to CO:Pd Loading Effect

GAO Dun-feng, YAN Cheng-cheng, WANG Guo-xiong*, BAO Xin-he*
(*State Key Laboratory of Catalysis, Dalian National Laboratory for Clean Energy, Dalian Institute of Chemical Physics, Chinese Academy of Sciences, Dalian*, 116023, *China*)

Abstract: Nanostructured heterogeneous catalysts have been widely used in the electrochemical carbon dioxide (CO_2) reduction reaction (CO_2RR), which can simultaneously achieve the electrocatalytic conversion of CO_2 to fuels and the storage of renewable energy sources. Carbon supported palladium nanoparticles (Pd/C) catalysts have been previously reported to show excellent CO_2RR performance. However, the crucial role of the metal loading in supported electrocatalysts has been rarely reported. In this work, we study the Pd loading effect on the structure of Pd/C catalysts as well as their activity and selectivity of CO_2RR to CO. The Pd loadings in Pd/C catalysts were well controlled by an effective liquid synthesis method. The Pd nanoparticles were homogeneously dispersed on the carbon support, and the Pd loading played a minor role in the particle size. The as-prepared Pd/C catalysts were studied in an optimized electrolyte, 0.1 mmol·L^{-1} $KHCO_3$. It shows a volcano relationship between CO Faradaic efficiency (FE) and the Pd loading, with the highest CO FE of 91.2% over the 20wt% Pd/C catalyst at -0.89 V versus the reversible hydrogen electrode (vs. RHE). The geometric CO partial current density had a positive correlation with the Pd loading, while the highest turnover frequency for CO production was observed over the 2.5wt% Pd/C catalyst (~ 918 h^{-1} at -0.89 V vs. RHE). The Pd loading effects on the activity and selectivity of CO_2RR to CO could be attributed to the number of active sites, reaction kinetics, and the stabilization of key intermediates, as well as the mass transport of reactants, intermediates and products. This work provides new insight into the loading effect, an important reactivity descriptor determining the CO_2RR performance.

Key words: electrochemical carbon dioxide reduction reaction; Pd/C catalysts; loading; electrolyte; selectivity
CLC Number: O646 **Document Code**: A

Electrochemical carbon dioxide (CO_2) reduction reaction (CO_2RR) to fuels and chemicals provides an effective approach which not only reduces the emission of environmentally harmful CO_2, but also provides means of storing intermittent electricity originating from renewable energy sources like wind, so lar, and hydro[1]. Nanostructured heterogeneous catalysts which have been widely explored show superior CO_2RR performance compared to their bulk counter part[2-13]. Among them, Pd and Pd-based nanostructures are verified to be the efficient catalysts for CO_2RR to formate, carbon monoxide (CO), hydrocarbons and alcohols[14-30]. The activity and selectivity of these catalysts are tuned by rationally engineering size effect[15], strain effect[17], shape effect[20], low-coordinated sites[18], as well as the geometric and electronic effects[28].

Apart from the structure and electronic property of a catalyst, other parameters such as the electrolyte composition and pH[31-34], the configuration of used cell[28, 35], as well as the metal loading of supported nanoparticles (NPs) catalyst[35-38] are also of importance to determine the activity and selectivity of CO_2RR. Carbon supported palladium NPs (Pd/C) catalysts can selectively reduce CO_2 to CO at high overpotentials[15, 23, 39]. Our previous work indicates that the production of CO over Pd NPs is dependent on the low-coordinate sites and active phase controlled by the applied potential and reaction intermediate[15, 39]. However, to the best of our knowledge, the loading effect of Pd/C catalysts on the CO_2RR to CO has not been reported so far. In this work, we prepared a series of Pd/C catalysts with different loadings and studied

Received: 2018-09-05, Revised: 2018-09-18 *Corresponding author, Tel: (86-411)84379976;(86-411)84379128, E-mail: wanggx@dicp.ac.cn;xhbao@dicp.ac.cn

the Pd loading effects on the activity and selectivity of CO_2RR performance. In the optimized electrolyte, 0.1 mol·L^{-1} $KHCO_3$, a volcano relationship between CO Faradaic efficiency (FE) and the loading was observed. The geometric CO partial current density showed a positive correlation with the Pd loading, while the highest turnover frequency (TOF) for CO production was observed over the 2.5wt% Pd/C catalyst. The loading effect could be attributed to the number of active sites, the stabilization of key intermediates, as well as the mass transport of reactants, intermediates and products.

1 Experimental Section

1.1 Catalysts Preparations

Pd/C catalysts were synthesized at room temperature in an aqueous solution with sodium borohydride ([$NaBH_4$], Sinopharm Chemical Reagent Co. Ltd.) as a reducing agent and sodium citrate ([$Na_3C_6H_5O_7·2H_2O$], Sinopharm Chemical Reagent Co. Ltd.) as a stabilizing agent[15]. The molar ratio of sodium citrate to $PdCl_2$ was 8 and the molar ratio of $NaBH_4$ to $PdCl_2$ was 10. The detailed preparation procedure for Pd/C-10% (with a Pd loading of 10wt%) was as follows: 0.25 mmol $PdCl_2$ (dissolved in 0.1 mol·L^{-1} HCl solution) and 1 mmol sodium citrate were dissolved into 200 mL water, and then 106.4 mg Vulcan XC-72R carbon black (Carbot Corp.) was added, and sonicated for 30 min. A 25 mL of $NaBH_4$ solution (0.1 mmol·L^{-1}) was added into the suspension dropwise under vigorous stirring. After the suspension was stirred for 8 h, the black precipitate was filtered, washed and dried overnight in a vacuum oven at room temperature. Other Pd catalysts with different Pd loading (2.5wt%, 5wt%, 20wt%, 30wt% and 40wt%) were also prepared with the same method.

1.2 Physicochemical Characterizations

The actual loading of Pd in Pd/C catalyst was measured by inductively coupled plasma optical emission spectroscopy (ICP-OES). Transmission electron microscopy (TEM) was carried out on a JEM-2100 microscope operated at an accelerating voltage of 200 kV. X-ray diffraction (XRD) was performed on a Rigaku D/MAX 2500 diffractometer with Cu K_α radiation (λ = 1.5418 Å) at 40 kV and 200 mA. The scan speed was 2°·min^{-1} and the step size was 0.02°. X-ray photoelectron spectroscopic (XPS) measurements were carried out using a Thermo Scientific Escalab 250Xi spectrometer with Al K_α X-ray as radiation source. The position of the C 1s peak, which is 284.6 eV, was used to correct the binding energy.

1.3 Electrode Preparation

Carbon black ink containing Vulcan XC-72R carbon black and polytetrafluoroethylene (PTFE, Sigma-Aldrich) was painted onto a piece of Toray carbon paper (Toray TGP-H-060, Toray Industries Inc.) to form a microporous layer. The carbon black loading was about 1 mg·cm^{-2} and the PTFE content in the microporous layer was 15wt%. To fabricate the catalyst layer, the as-prepared catalyst and Nafion ionomer solution (5wt%, DuPont) were ultrasonically suspended in a water/alcohol mixture and then brushed onto the microporous layer. The loading of Pd/C catalyst was 2.0 ± 0.1 mg·cm^{-2}, and the Nafion content in the catalyst layer was 10wt%.

1.4 Electrochemical Measurements

Electrochemical measurements were carried out in an H-cell separated by a Nafion 115 membrane. The Pt wire and Ag/AgCl electrode were used as the counter electrode and reference electrode, respectively. A piece of the Toray carbon fiber paper with the catalyst layer (1 cm × 2 cm) was used as the working electrode. The samples were measured with a chronoamperometric step for 30 min at each potential, and the potentials were controlled with an Autolab potentiostat (PGSTAT 302N). All potentials in this study were measured against an Ag/AgCl reference electrode and converted to the reversible hydrogen electrode (RHE) reference scale by E(vs. RHE) = E (vs. Ag/AgCl) + 0.21 V + 0.0591 × pH. CO_2RR was conducted in CO_2-saturated 0.1 mmol·L^{-1} $KHCO_3$ (pH 6.8), 0.1 mol·L^{-1} $NaHCO_3$ (pH 6.8) and 0.05 mol·L^{-1} K_2SO_4 (pH 4.2) solutions at room temperature and under atmospheric pressure. Prior to the measurement, the electrolyte was bubbled by 5% N_2/CO_2 (20 mL·min^{-1}, N_2 as an internal standard for the quantification) for 30 min to remove residual air in the solution and satu-

rate the solution. The gas products were monitored by an on line micro gas chromatography (GC, Agilent 490) equipped with a TCD detector and Molsieve 5A column once every three minutes. The liquid product was analyzed on a Varian 400 MHz nuclear magnetic resonance (NMR) spectrometer after the reaction. The ^{1}H spectrum was measured with water suppression by a pre-saturation method. The calculation of TOF was previously described in our work[15].

2 Results and Discussion

Pd/C catalysts with different Pd loadings were synthesized with sodium borohydride as a reducing agent and sodium citrate as a stabilizing agent. The Pd loading was controlled by tuning the weight ratio of $PdCl_2$ precursor and carbon black support. As shown in Table 1, the actual loadings of the as-prepared Pd/C catalysts, determined by the ICP-OES, were close to the nominal loadings. The morphology of the as-prepared Pd/C catalysts was characterized by TEM, as shown in Figures 1A-F. Pd NPs were homogeneously dispersed on the carbon support and the density of NPs obviously increased with the Pd loading. The Pd NPs were found to be slightly agglomerated in the case of a high Pd loading, Pd/C-30% and Pd/C-40% (Figures 1E-F). Figure 1G shows the size distributions of Pd NPs in the above Pd/C catalysts, which were determined by counting more than 200 particles from TEM images acquired in several randomly selected regions. Although the molar ratio of sodium citrate and $PdCl_2$ was kept at 8 for all the samples during the preparation, the average NPs size still increased from 2.3 nm in Pd/C-2.5% to 4.0 nm in Pd/C-40% (Figure 1H). However, as we have previously reported, Pd NPs in this size range (2.3 ~ 4.0 nm) showed high apparent CO_2RR performance and no remarkable size effect[15], therefore, the difference in the catalytic performance (will be shown later) can be mainly attributed to the loading effect.

The XRD patterns of the as-prepared Pd/C catalysts are shown in Figure 2A. The peaks at 40.1°, 46.7°, 68.1°, 82.1° and 86.6° were the characteristic (111), (200), (220), (311) and (222) planes of metallic Pd with a face-centered cubic (fcc) structure (JCPDS: 65-6174). There were no obvious diffraction peaks that could be assigned to palladium oxides. The slightly sharpened peaks with the increased loading suggested an increased NPs size, consistent with statistical results from TEM images. The surface composition of the Pd NPs in the as-prepared Pd/C catalysts was characterized by XPS. Figure 2B shows the high resolution Pd 3d spectra of the Pd/C-20% catalyst. The peaks at 355.6 and 340.9 eV were assigned to the metallic Pd, while the peaks at 336.9 and 342.2 eV were assigned to the surface Pd(II)O with 54.2at% in all the Pd species, which could be formed by the re-oxidation of the as-synthesized Pd NPs in the air and could be not detected by XRD (Figure 2A). The assignment of the Pd 3d spectra was consistent with those of carbon supported Pd NPs in the literature[19,40]. It should be noted that the palladium oxide on the surface does not play a role in the CO_2RR since it would be reduced to form metallic Pd or Pd hydride under reducing conditions[23,39,41].

Tab. 1 The nominal and actual Pd loadings of Pd/C catalysts

Catalyst	Pd loading/wt%	
	Nominal	Actual
Pd/C-2.5%	2.5	2.1
Pd/C-5%	5	4.7
Pd/C-10%	10	9.9
Pd/C-20%	20	18.6
Pd/C-30%	30	27.4
Pd/C-40%	40	37.3

CO_2RR performance was evaluated in an H-cell with a chronoamperometric measurement, and the gas and liquid products were analyzed by an on line GC and ^{1}H-NMR, respectively. In all the experiments in this work, CO and H_2 are the only gas products and a trace amount of formate was also detected (~ 1% FE, not shown). Firstly, we studied the electrolyte effect on the CO_2RR performance over Pd/C-20%, as shown in Figure 3. At less negative potentials below -0.89 V vs. RHE, the Pd/C-20% catalyst measured in the $KHCO_3$ solution showed the highest CO FE, probably attributed to the promoter effect of larger cations (K^+

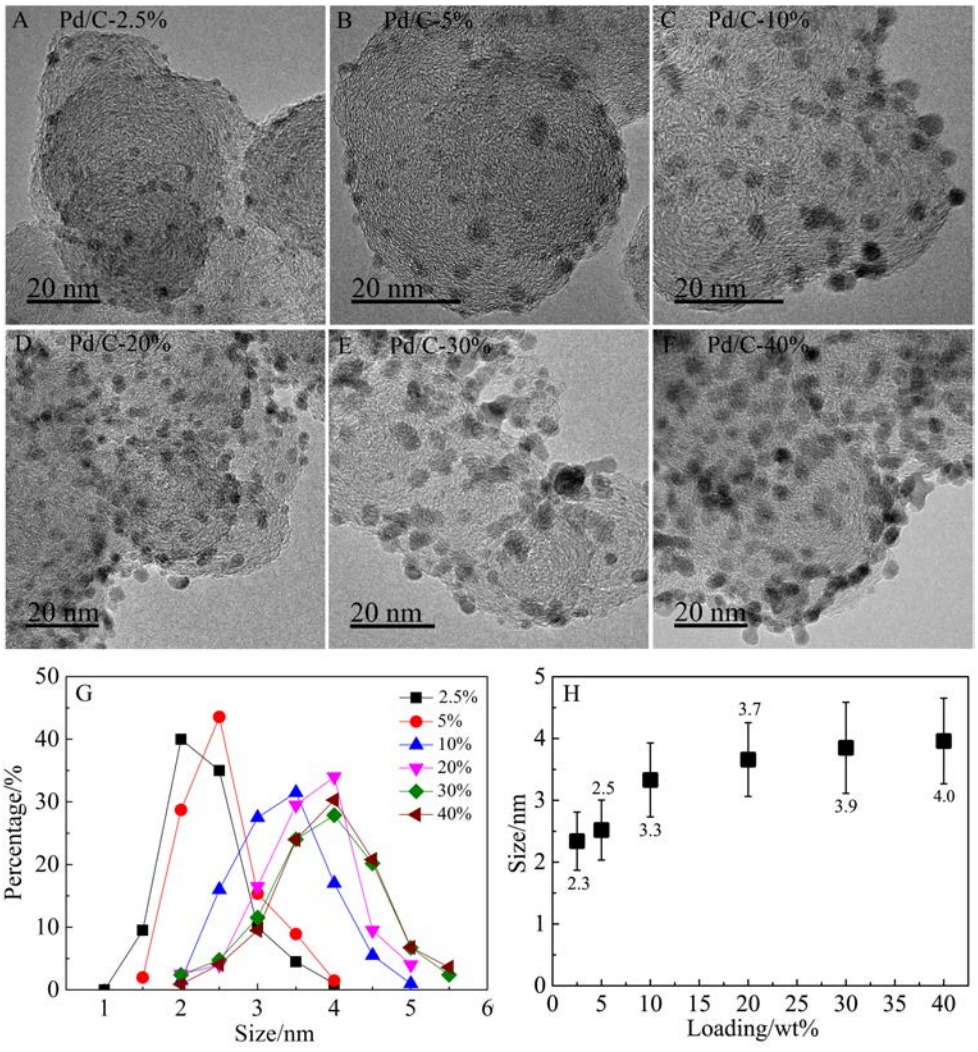

Fig. 1 TEM images of Pd/C catalysts with different loadings: (A) 2.5%, (B) 5%, (C) 10%, (D) 20%, (E) 30% and (F) 40%; (G) Size distributions of the Pd/C catalysts; (H) Loading dependence of the size of Pd NPs.

vs. Na^+) on the formation of the COOH* and CO* intermediates[31] as well as the higher effective CO_2 concentration near the electrode surface (HCO_3^- vs. SO_4^{2-}) which was enhanced by the fast equilibrium between the bicarbonate anion and the dissolved CO_2 molecule[32]. In contrast, the Pd/C-20% catalyst measured in the K_2SO_4 solution showed the highest CO FE (thus, the lowest H_2 FE) at more negative potentials above -0.99 V vs. RHE, where the reaction was usually controlled by the mass transport of CO_2. The suppressed hydrogen evolution reaction was attributed to the higher local pH near the electrode in K_2SO_4 versus $KHCO_3$, which was considered as a weak buffer solution. However, the Pd/C-20% catalyst measured in the $KHCO_3$ solution showed the highest partial current density for CO production in the whole potential range (Figure 3B), suggesting that $KHCO_3$ is the optimum electrolyte for CO_2RR over Pd/C catalysts.

As we discussed above, the 0.1 mmol·L^{-1} $KHCO_3$ solution was used as the electrolyte for studying the Pd loading effect. As shown in Figure 4A, CO FE increased with the Pd loading from 2.5wt% to 20wt%, slightly decreased when further increasing it to 30wt%, and obviously decreased with 40wt% loading especially at more negative potentials. The geometric CO partial current density showed that the reaction rate of CO_2RR to CO increased with the Pd loading (Figure 4B). Interestingly, by decreasing the loading to 2.5wt%, an ultrahigh mass activity for CO production (-98.1 A·g^{-1}_{Pd} at -0.89 V vs. RHE and -252 A·g^{-1}_{Pd} at

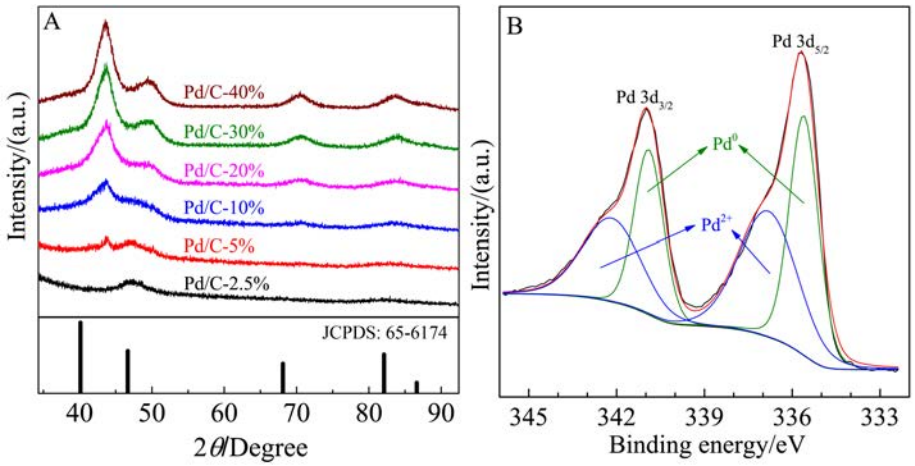

Fig. 2 (A). XRD patterns of Pd/C catalysts with different loadings; (B). Pd 3d XPS spectra of the Pd/C-20% catalyst

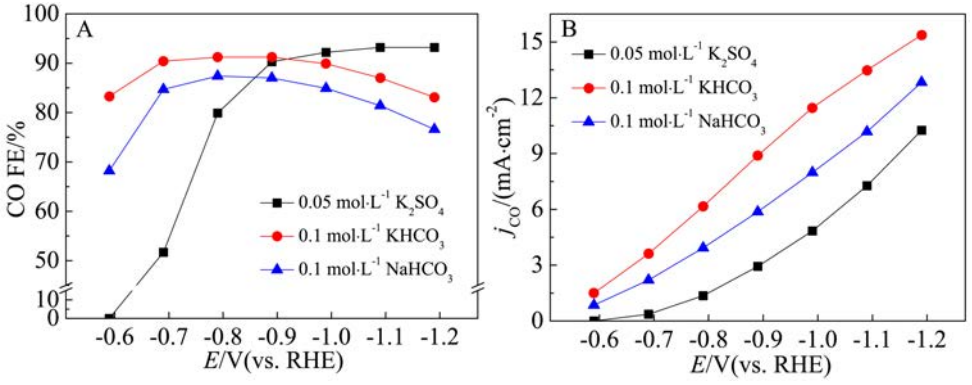

Fig. 3 Applied potential dependence of (A) Faradaic efficiencies and (B) geometric partial current densities for CO production over Pd/C-20% in CO_2-saturated 0.1 mmol·L^{-1} $KHCO_3$, 0.1 mmol·L^{-1} $NaHCO_3$ and 0.05 mmol·L^{-1} K_2SO_4 solutions.

-1.19 V vs. RHE, in Figure 4C) was obtained compared to the literature[14]. In order to show a clear loading-reactivity correlation, we compared the loading dependence of FE and geometric partial current density for CO production at -0.89 V vs. RHE (Figure 4D), where the highest CO FEs were reached over most of the Pd/C catalysts and the CO_2RR performance was less affected by the mass transport compared to that at more negative potentials. The CO FE increased from 73.3% over Pd/C-2.5% to 91.2% over Pd/C-20% and then decreased to 79.6% over Pd/C-40%. Therefore, 20wt% is considered to be an optimum Pd loading of the Pd/C catalysts for CO_2RR, as reported in our previous work[15,34,39,41-42]. The selectivity variation between CO and H_2 with the Pd loading could be attributed to the stabilization of key intermediates affected by a distinct potential distribution in the electric double layer[43-45] between NPs as well as the mass transport of reactants, intermediates and products at the mesoscale[36-37]. The slight agglomeration of Pd NPs of Pd/C catalysts with a high loading could also cause the decrease of CO FE. The monotonic increase of CO partial current density with the Pd loading (Figure 4D) demonstrates the presence of more active sites provided by the increased loading[35].

In order to study the intrinsic loading effect and better decouple it from the increased number of active sites, we calculated the TOF for CO production over different Pd/C catalysts in the light of our previous understanding that the edge and corner sites of Pd NPs have been theoretically proposed to be the active sites for CO_2RR to CO[15]. As shown in Figure 5, the TOF for CO production increased with decreasing the Pd loading, in clear contrast with the positive

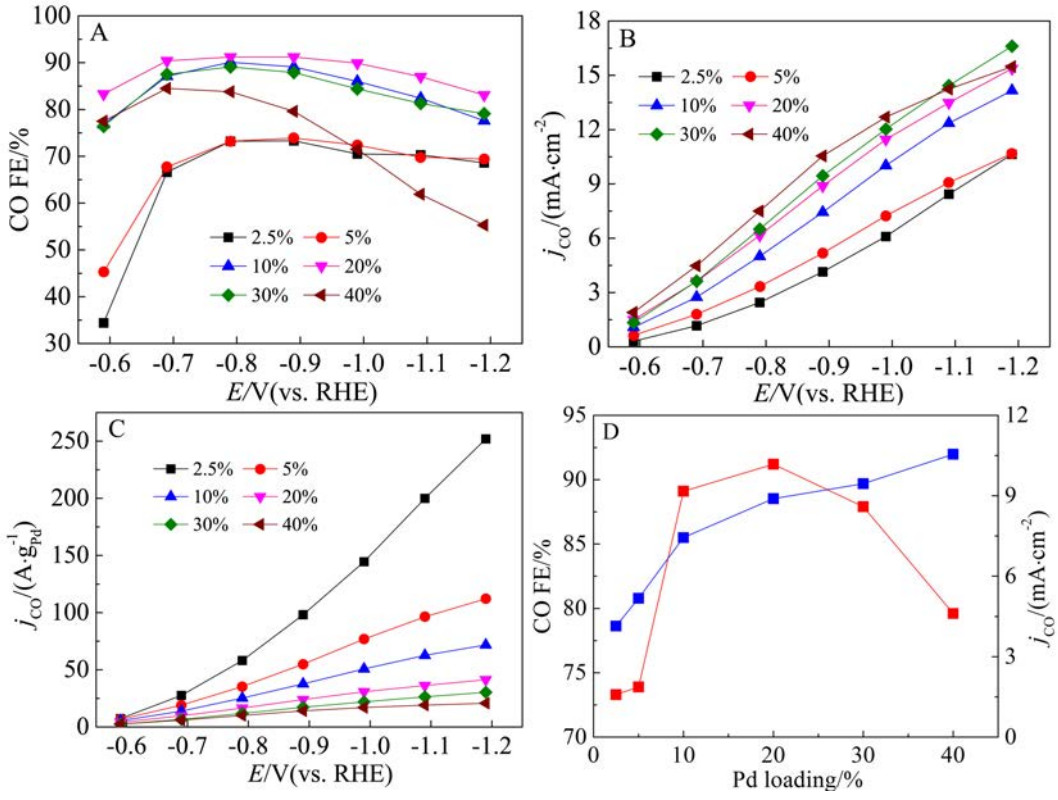

Fig. 4 Applied potential dependence of (A) Faradaic efficiencies, (B) geometric partial current densities and (C) mass normalized current densities for CO production over Pd/C catalysts with different loadings in a CO_2-saturated 0.1 mmol·L^{-1} $KHCO_3$ solution; (D) Loading dependence of Faradaic efficiencies and geometric partial current densities for CO production at -0.89 V vs. RHE.

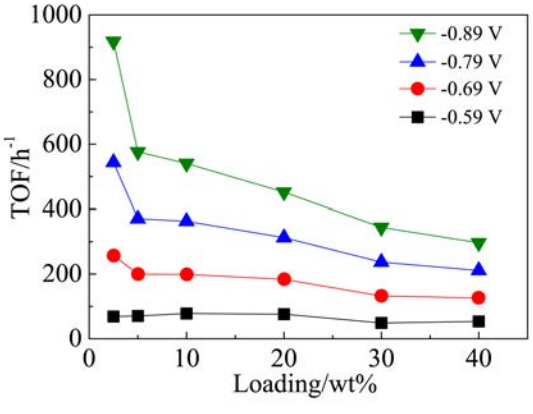

Fig. 5 Loading dependence of turnover frequency (TOF) for CO production over Pd/C catalysts at various potentials in a CO_2-saturated 0.1 mmol·L^{-1} $KHCO_3$ solution.

correlation between CO partial current density and the loading. The highest TOF for CO production (~ 918 h^{-1}) was achieved over Pd/C-2.5% at -0.89 V vs. RHE. The high intrinsic activity of Pd/C catalysts with very low loading was probably attributed to the enhanced reaction kinetics in the local environment near the surface of a single particle[46-47].

3 Conclusions

In summary, the Pd/C catalysts with different Pd loadings were successfully synthesized by a facile liquid reduction method. The Pd nanoparticles were dispersed on the carbon support, and the Pd loading played a minor role in the particle size. The as-prepared Pd/C catalysts were studied in an optimized electrolyte, 0.1 mmol·L^{-1} $KHCO_3$. It shows a volcano relationship between CO FE and the Pd loading, with the highest CO FE of 91.2% over the 20wt% Pd/C catalyst at -0.89 V vs. RHE. The geometric CO partial current density showed a positive correlation with the Pd loading, while the highest TOF for CO production was observed over the 2.5wt% Pd/C catalyst. The Pd loading effect on the activity and selectivity of CO_2RR to CO could be attributed to the number of

active sites, reaction kinetics, and the stabilization of key intermediates, as well as the mass transport of reactants, intermediates and products. This work provides new insight into the loading effect, an important reactivity descriptor determining the CO_2RR performance.

Acknowledgments

We gratefully acknowledge financial support from the Ministry of Science and Technology of China (Grant 2017YFA 0700102), the National Natural Science Foundation of China (Grants 21573222 and 91545202), Outstanding Youth Talent Project of Dalian (2017RJ03), Dalian Institute of Chemical Physics (Grant DICP DMTO201702), the Strategic Priority Research Program of the Chinese Academy of Sciences (Grant No. XDB17020200). G.X. Wang thanks the financial support from CAS Youth Innovation Promotion (Grant No. 2015145).

References:

[1] Montoya J H, Seitz L C, Chakthranont P, et al. Materials for solar fuels and chemicals[J]. Nature Materials, 2017, 16 (1): 70-81.

[2] Gao D F, Cai F, Wang G X, et al. Nanostructured heterogeneous catalysts for electrochemical reduction of CO_2[J]. Current Opinion in Green and Sustainable Chemistry, 2017, 3: 39-44.

[3] Zhu D D, Liu J L, Qiao S Z. Recent advances in inorganic heterogeneous electrocatalysts for reduction of carbon dioxide[J]. Advanced Materials, 2016, 28(18): 3423-3452.

[4] Larrazábal G O, Martín A J, Pérez-Ramírez J. Building blocks for high performance in electrocatalytic CO_2 reduction: materials, optimization strategies, and device engineering[J]. The Journal of Physical Chemistry Letters, 2017, 8(16): 3933-3944.

[5] Wang Y H, Liu J L, Wang Y F, et al. Tuning of CO_2 reduction selectivity on metal electrocatalysts[J]. Small, 2017, 13 (43): 1701809.

[6] Zhou J H, Zhang Y. Metal-based heterogeneous electrocatalysts for reduction of carbon dioxide and nitrogen: mechanisms, recent advances and perspective[J]. Reaction Chemistry & Engineering, 2018, 3: 591-625.

[7] Zhuang T T, Liang Z Q, Seifitokaldani A, et al. Steering post-C-C coupling selectivity enables high efficiency electroreduction of carbon dioxide to multi-carbon alcohols[J]. Nature Catalysis, 2018, 1(6): 421-428.

[8] Gao D F, Zhang Y, Zhou Z W, et al. Enhancing CO_2 electroreduction with the metal-oxide interface[J]. Journal of the American Chemical Society, 2017, 139(16): 5652-5655.

[9] Gao S, Lin Y, Jiao X C, et al. Partially oxidized atomic cobalt layers for carbon dioxide electroreduction to liquid fuel[J]. Nature, 2016, 529(7584): 68-71.

[10] Jiang B(蒋宇), Zhang L N(张莉娜), Qin X X(秦先贤), et al. Electrodeposition of RuO_2 layers on TiO_2 nanotube array toward CO_2 electroreduction[J]. Journal of the Electrochemistry(电化学), 2017, 23(2): 238-244.

[11] Xie H, Wang T Y, Liang J S, et al. Cu-based nanocatalysts for electrochemical reduction of CO_2[J]. Nano Today, 2018, 21: 41-54.

[12] Yan C C, Li H B, Ye Y F, et al. Coordinatively unsaturated nickel-nitrogen sites towards selective and high-rate CO_2 electroreduction[J]. Energy & Environmental Science, 2018, 11(5): 1204-1210.

[13] Wang X Q, Chen Z, Zhao X Y, et al. Regulation of coordination number over single Co sites: Triggering the efficient electroreduction of CO_2[J]. Angewandte Chemie International Edition, 2018, 57(7): 1944-1948.

[14] Gao D F, Zhou H, Cai F, et al. Pd-containing nanostructures for electrochemical CO_2 reduction reaction[J]. ACS Catalysis, 2018, 8(2): 1510-1519.

[15] Gao D F, Zhou H, Wang J, et al. Size-dependent electrocatalytic reduction of CO_2 over Pd nanoparticles[J]. Journal of the American Chemical Society, 2015, 137 (13): 4288-4297.

[16] Min X, Kanan M W. Pd-catalyzed electrohydrogenation of carbon dioxide to formate: high mass activity at low overpotential and identification of the deactivation pathway[J]. Journal of the American Chemical Society, 2015, 137(14): 4701-4708.

[17] Huang H W, Jia H H, Liu Z, et al. Understanding of strain effects in the electrochemical reduction of CO_2: using Pd nanostructures as an ideal platform[J]. Angewandte Chemie International Edition, 2017, 56(13): 3594-3598.

[18] Zhu W J, Zhang L, Yang P P, et al. Low-coordinated edge sites on ultrathin palladium nanosheets boost carbon dioxide electroreduction performance[J]. Angewandte Chemie International Edition, 2018, 57(36): 11544-11548.

[19] Jiang B, Zhang X G, Jiang K, et al. Boosting formate production in electrocatalytic CO_2 reduction over wide potential window on Pd surfaces[J]. Journal of the American Chemical Society, 2018, 140(8): 2880-2889.

[20] Klinkova A, De Luna P, Dinh C T, et al. Rational design of efficient palladium catalysts for electroreduction of carbon dioxide to formate[J]. ACS Catalysis, 2016, 6(12): 8115-8120.

[21] Zhou F L, Li H T, Fournier M, et al. Electrocatalytic CO_2 reduction to formate at low overpotentials on electrode-

posited Pd films: stabilized performance by suppression of CO formation[J]. ChemSusChem, 2017, 10(7): 1509-1516.

[22] Rahaman M, Dutta A, Broekmann P. Size-dependent activity of palladium nanoparticles: efficient conversion of CO_2 into formate at low overpotentials[J]. ChemSusChem, 2017, 10(8): 1733-1741.

[23] Sheng W C, Kattel S, Yao S Y, et al. Electrochemical reduction of CO_2 to synthesis gas with controlled CO/H_2 ratios[J]. Energy & Environmental Science, 2017, 10(5): 1180-1185.

[24] Zhang W Y, Qin Q, Dai L, et al. Electrochemical reduction of carbon dioxide to methanol on hierarchical Pd/SnO_2 nanosheets with abundant Pd-O-Sn interfaces[J]. Angewandte Chemie International Edition, 2018, 57(30): 9475-9479.

[25] Bai X F, Chen W, Zhao C C, et al. Exclusive formation of formic acid from CO_2 electroreduction by a tunable Pd-Sn alloy[J]. Angewandte Chemie International Edition, 2017, 56(40): 12219-12223.

[26] Zhang F Y, Sheng T, Tian N, et al. Cu overlayers on tetrahexahedral Pd nanocrystals with high-index facets for CO_2 electroreduction to alcohols[J]. Chemical Communications, 2017, 53(57): 8085-8088.

[27] Tao H C, Sun X F, Back S, et al. Doping palladium with tellurium for the highly selective electrocatalytic reduction of aqueous CO_2 to CO[J]. Chemical Science, 2018, 9 (2): 483-487.

[28] Ma S, Sadakiyo M, Heim M, et al. Electroreduction of CO_2 to hydrocarbons using bimetallic Cu-Pd catalysts with different mixing patterns[J]. Journal of the American Chemical Society, 2017, 139(1): 47-50.

[29] Kortlever R, Peters I, Balemans C, et al. Palladium-gold catalyst for the electrochemical reduction of CO_2 to C_1-C_5 hydrocarbons[J]. Chemical Communications, 2016, 52 (67): 10229-10232.

[30] Yin Z, Gao D F, Yao S Y, et al. Highly selective palladium-copper bimetallic electrocatalysts for the electrochemical reduction of CO_2 to CO[J]. Nano Energy, 2016, 27: 35-43.

[31] Gao D F, McCrum I T, Deo S, et al. Activity and selectivity control in CO_2 electroreduction to multicarbon products over CuO_x catalysts via electrolyte design[J]. ACS Catalysis, 2018, 8(11):10012-10020.

[32] Dunwell M, Lu Q, Heyes J M, et al. The central role of bicarbonate in the electrochemical reduction of carbon dioxide on gold[J]. Journal of the American Chemical Society, 2017, 139(10): 3774-3783.

[33] Gao D, Scholten F, Roldan Cu enya, B. Improved CO_2 electroreduction performance on plasma-activated Cu catalysts via electrolyte design: Halide effect[J]. ACS Catalysis, 2017, 7(8): 5112-5120.

[34] Gao D F, Wang J, Wu H H, et al. pH Effect on electrocatalytic reduction of CO_2 over Pd and Pt nanoparticles [J]. Electrochemistry Communications, 2015, 55: 1-5.

[35] Del Castillo A, Alvarez-Guerra M, Solla-Gullón J, et al. Electrocatalytic reduction of CO_2 to formate using particulate Sn electrodes: Effect of metal loading and particle size[J]. Applied Energy, 2015, 157: 165-173.

[36] Mistry H, Behafarid F, Reske R, et al. Tuning catalytic selectivity at the mesoscale via interparticle interactions [J]. ACS Catalysis, 2016, 6(2): 1075-1080.

[37] Wang X L, Varela A S, Bergmann A, et al. Catalyst particle density controls hydrocarbon product selectivity in CO_2 electroreduction on CuO_x[J]. ChemSusChem, 2017, 10(22): 4642-4649.

[38] Yu J L, Liu H Y, Song S Q, et al. Electrochemical reduction of carbon dioxide at nanostructured SnO_2/carbon aerogels: The effect of tin oxide content on the catalytic activity and formate selectivity[J]. Applied Catalysis A: General, 2017, 545: 159-166.

[39] Gao D F, Zhou H, Cai F, et al. Switchable CO_2 electroreduction via engineering active phases of Pd nanoparticles [J]. Nano Research, 2017, 10(6): 2181-2191.

[40] Lv Q, Meng Q L, Liu W W, et al. Pd-PdO interface as active site for HCOOH selective dehydrogenation at ambient condition[J]. The Journal of Physical Chemistry C, 2018, 122(4): 2081-2088.

[41] Cai F, Gao D F, Zhou H, et al. Electrochemical promotion of catalysis over Pd nanoparticles for CO_2 reduction [J]. Chemical Science, 2017, 8(4): 2569-2573.

[42] Cai F, Gao D F, Si R, et al. Effect of metal deposition sequence in carbon-supported Pd-Pt catalysts on activity towards CO_2 electroreduction to formate[J]. Electrochemistry Communications, 2017, 76: 1-5.

[43] Nesselberger M, Roefzaad M, Fayçal Hamou R, et al. The effect of particle proximity on the oxygen reduction rate of size-selected platinum clusters[J]. Nature Materials, 2013, 12(10): 919-924.

[44] Taylor S, Fabbri E, Levecque P, et al. The Effect of platinum loading and surface morphology on oxygen reduction activity[J]. Electrocatalysis, 2016, 7(4): 287-296.

[45] Antolini E. Structural parameters of supported fuel cell catalysts: The effect of particle size, inter-particle distance and metal loading on catalytic activity and fuel cell performance[J]. Applied Catalysis B: Environmental, 2016, 181: 298-313.

[46] Hauff K, Tuttlies U, Eigenberger G, et al. A global description of DOC kinetics for catalysts with different platinum loadings and aging status[J]. Applied Catalysis B: Environmental, 2010, 100(1/2): 10-18.

[47] Kang S B, Han S J, Nam S B, et al. Activity function describing the effect of Pd loading on the catalytic performance of modern commercial TWC[J]. Chemical Engineering Journal, 2012, 207(SI): 117-121.

Pd/C 催化剂用于 CO_2 电化学还原生成 CO:Pd 载量的影响

高敦峰,阎程程,汪国雄*,包信和*

(中国科学院大连化学物理研究所,大连洁净能源国家实验室,催化基础国家重点实验室, 辽宁 大连 116023)

摘要: CO_2 电化学还原反应可以将 CO_2 转化为燃料并同时实现再生能源的有效存储. 目前纳米结构的多相催化剂已经广泛应用于此反应,其中碳负载钯纳米粒子(Pd/C)表现出优异的 CO_2 电化学还原性能. 本工作研究了钯载量对于 Pd/C 催化剂结构以及其催化 CO_2 还原生成 CO 反应活性和选择性的影响. 不同载量的 Pd/C 催化剂通过液相还原方法制备,钯纳米粒子均匀地分散在碳载体上,载量并没有明显改变对纳米粒子的粒径. 在优选的电解质(0.1 mol·L^{-1} $KHCO_3$)中,CO 法拉第效率与载量呈现火山型曲线关系,-0.89 V 时载量为 20wt%的 Pd/C 催化剂达到最高的 CO 法拉第效率(91.2%). 生成 CO 的几何电流密度随着钯载量的增加而增加,但 CO 转换频率具有相反的趋势,载量为 2.5wt%的 Pd/C 催化剂具有最高的转换频率. 这种载量对 CO_2 电化学还原反应活性和选择性的影响主要由活性位的数量、反应动力学、中间物种的稳定性以及反应物、中间物种和产物的传质过程等共同决定.

关键词: CO_2 电化学还原;Pd/C 催化剂;载量;电解质;选择性